Mechanism of Inhibition of Human KSP by *Ispinesib*

Latesh Lad,*,‡ Lusong Luo,§ Jeffrey D. Carson,§ Kenneth W. Wood,‡ James J. Hartman,‡ Robert A. Copeland,§ and Roman Sakowicz‡

Department of Enzymology and Mechanistic Pharmacology, GlaxoSmithKline, Collegeville, Pennsylvania 19426, and Cytokinetics Inc., 280 East Grand Avenue, South San Francisco, California 94080

Received October 14, 2007; Revised Manuscript Received January 16, 2008

ABSTRACT: KSP, also known as HsEg5, is a kinesin that plays an essential role in the formation of a bipolar mitotic spindle and is required for cell cycle progression through mitosis. *Ispinesib* is the first potent, highly specific small-molecule inhibitor of KSP tested for the treatment of human disease. This novel anticancer agent causes mitotic arrest and growth inhibition in several human tumor cell lines and is currently being tested in multiple phase II clinical trials. In this study we have used steady-state and pre-steady-state kinetic assays to define the mechanism of KSP inhibition by *ispinesib*. Our data show that *ispinesib* alters the ability of KSP to bind to microtubules and inhibits its movement by preventing the release of ADP without preventing the release of the KSP−ADP complex from the microtubule. This type of inhibition is consistent with the physiological effect of *ispinesib* on cells, which is to prevent KSP-driven mitotic spindle pole separation. A comparison of *ispinesib* to monastrol, another small-molecule inhibitor of KSP, reveals that both inhibitors share a common mode of inhibition.

Kinesin motor proteins utilize the energy from ATP[1] hydrolysis to transport cellular cargo along microtubules. Over the past decade, kinesins that play essential roles in the mechanics of mitosis have become attractive targets for novel antimitotic cancer therapies because their known functions are limited to dividing cells. Drugs that perturb mitosis (antimitotics) are effective in the treatment of many cancers (*1*). The antimitotic agents in clinical use today all act on microtubules (MTs). However, since microtubules are essential for many cellular processes in nondividing cells, these agents cause corresponding undesirable toxicities in normal cells. Targeting mitotic kinesins offers an alternative and attractive path in the discovery of novel and specific antimitotic drugs for the treatment of cancer because they should not disrupt microtubule-based cellular processes unrelated to proliferation, such as neuronal transport (*2*).

KSP is a human member of the kinesin-5 subfamily. It is a plus-end-directed kinesin that localizes to interpolar spindle microtubules and to the spindle poles and is required for normal spindle function (*3–8*). Unlike the kinesin-1 motors, which move vesicles along microtubules, KSP and the other kinesin-5 members have a unique structure appropriate for bringing about relative motions of the microtubules themselves. They accomplish this through their bipolar homotetrameric structure which places two pairs of motor domains at each end of an extended stalk, enabling KSP to cross-link microtubules and induce MT−MT sliding during centrosome separation in the formation of the bipolar spindle (*3, 6, 7*). Monastrol is the first specific small molecule inhibitor of the vertebrate kinesin-5 subfamily (*9–13*). It is cell-permeable, and its effect on dividing cells is to bring about collapse of pre-existing bipolar spindles and cell cycle arrest with a monopolar spindle, which is nearly identical to the phenotype observed when KSP is inhibited by anti-KSP antibodies (*10, 14, 15*). Monastrol is not competitive with ATP but is competitive with MTs in inhibition of the KSP ATPase (*16*). The cocrystal structure of the monastrol-bound KSP motor domain complex revealed that monastrol is indeed an allosteric inhibitor that binds to an induced-fit pocket 12 Å away from the nucleotide binding pocket. Further comparison of the bound and unbound inhibitor structures showed that the binding of monastrol triggers a downward swing of the insertion loop (loop L5) between helix α2 and helix α3, generating a binding pocket which is also accompanied by structural changes in the switch I and switch II regions of the protein (*13*). Initially, a detailed pre-steady-state kinetic analysis showed that monastrol stabilizes a conformation of KSP that favors ATP resynthesis after ATP hydrolysis, altering the ability of KSP to generate force and diminishing its ability to establish or maintain the bipolar spindle (*17*). However, a more recent study suggests that there is no kinetic evidence supporting monastrol-stimulated ATP resynthesis in the absence or presence of MT (*18*).

In this study, we investigate in detail the mechanism of inhibition of KSP by *ispinesib* in the presence and absence of MT utilizing both steady-state and transient-state kinetic techniques. *Ispinesib* is a quinazolinone inhibitor of KSP currently being studied in multiple phase II clinical trials. *Ispinesib* was identified by screening a collection of small

* To whom correspondence should be addressed. E-mail: llad@cytokinetics.com. Phone: (650) 624-3000. Fax: (650) 624-3010.

‡ Cytokinetics Inc.

§ GlaxoSmithKline.

[1] Abbreviations: KSP, human kinesin spindle protein; ATP, adenosine 5′-triphosphate; AMP-PNP, adenosine 5′-(β,γ-imido)triphosphate; ADP, adenosine 5′-diphosphate; MT, microtubule; EGTA, ethylene glycol *O*,*O*′-bis(2-aminoethyl)-*N*,*N*,*N*′,*N*′-tetraacetic acid; MDCC-PBP, 7-diethylamino-3-[[[2-(maleimidyl)ethyl]amino]carbonyl]coumarin-labeled phosphate binding protein; PNPase, purine nucleotide phosphorylase; MEG, methylguanosine; P_i, inorganic phosphate; PDRM, phosphodeoxyribomutase.

10.1021/bi702061g CCC: $40.75
Published on Web 02/22/2008

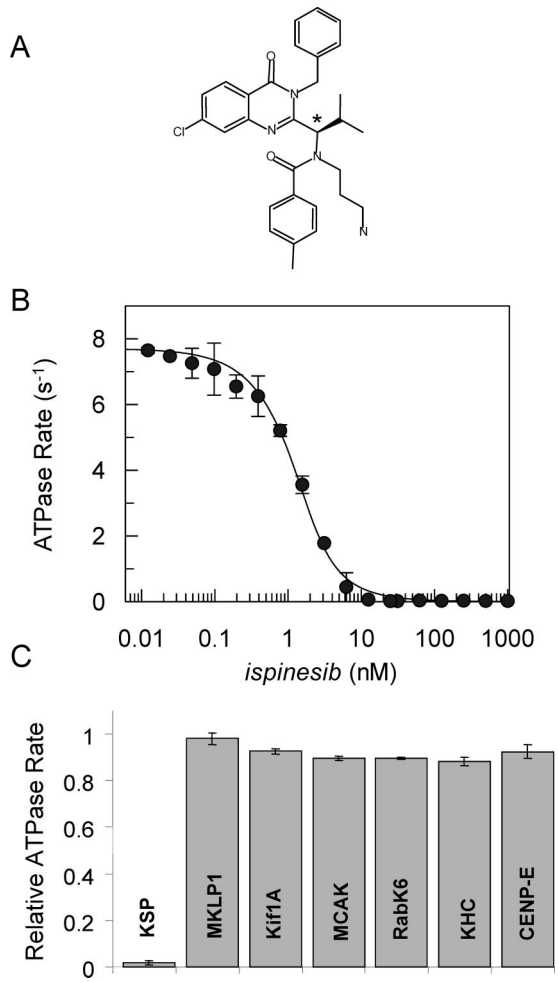

FIGURE 1: Structure and specificity of *ispinesib*. (A) *ispinesib* structure, with a single chiral center indicated by the asterisk. (B) Inhibition of MT-stimulated KSP ATPase activity by *ispinesib*. The reaction contained 0.75 nM KSP, 5 μM MT, and 500 μM ATP. (C) MT-stimulated ATPase rates of human kinesins in the presence of *ispinesib* (20 μM) normalized to rates observed in the absence of inhibitor.

synthetic organic compounds for inhibitors of KSP ATPase activity followed by synthetic chemical optimization to improve the compound's potency and drug-like properties. Preclinical data have revealed that *ispinesib* is efficacious in a number of mouse models of cancer and, unlike inhibitors that target microtubules or tubulin, did not exhibit neurotoxcity in these models (*19*). We find that *ispinesib* alters the ability of KSP to bind to MTs and inhibits its movement by slowing the release of ADP without trapping the MT−KSP−ADP intermediate. We also find no kinetic evidence indicating that *ispinesib* stabilizes the KSP ATP hydrolysis conformation such that it prompts ATP resynthesis. Comparison of our findings for *ispinesib* with the most recent data available for monastrol (*17, 18*) suggests that the molecular basis for KSP inhibition is almost identical for both inhibitors.

EXPERIMENTAL PROCEDURES

Expression and Purification. The motor domains of KSP (amino acids 1–360), MKLP1 (amino acids 4–433), CENP-E (amino acids 2–340), Kif1A (amino acids 3–353), MCAK (amino acids 257–617), and RabK6 (amino acids 59–506) were expressed in *Escherichia coli* BL21(DE3) as C-terminal 6-His fusion proteins. Bacterial pellets were lysed with a microfluidizer (Microfluidics Corp.) in lysis buffer [50 mM Tris-HCl, 50 mM KCl, 10 mM imidazole, 2 mM $MgCl_2$, 8 mM β-mercaptoethanol, 0.1 mM ATP (pH 7.4)], and the resulting proteins were further purified using Ni-NTA agarose affinity chromatography, with an elution buffer consisting of 50 mM PIPES, 10% sucrose, 300 mM imidazole, 50 mM KCl, 2 mM $MgCl_2$, 8 mM β-mercaptoethanol, and 0.1 mM ATP (pH 6.8).

Steady-State Kinetic Analysis of Human KSP ATPase Activity and Inhibition by Ispinesib. Kinesin specificity analysis was carried out using a pyruvate kinase−lactate dehydrogenase detection system that couples the production of ADP to oxidation of NADH (*21*). Absorbance changes were monitored at 340 nm. Steady-state studies using nanomolar concentrations of KSP were performed using a sensitive fluorescence-based assay utilizing a pyruvate kinase, pyruvate oxidase, and horseradish peroxidase coupled detection system that couples the generation of ADP to oxidation of Amplex Red to fluorescent resorufin. Generation of resorufin was monitored by fluorescence ($\lambda_{excitation} = 520$ nm and $\lambda_{emission} = 580$ nm). Steady-state biochemical experiments were performed in PEM25 buffer [25 mM Pipes-K^+ (pH 6.8), 2 mM $MgCl_2$, 1 mM EGTA] supplemented with 10 μM paclitaxel for experiments involving microtubules. The IC_{50} for steady-state inhibition was determined at 500 μM ATP, 5 μM MTs, and 1 nM KSP in PEM25 buffer. $K_{i\,app}$ (apparent inhibitor dissociation constant) estimates of *ispinesib* were extracted from the concentration–response curves, with explicit correction for enzyme concentration by using the Morrison equation (*20*):

$$\frac{v}{v_0} = 1 - \frac{([E] + [I] + K_{i\,app}) - \sqrt{([E] + [I] + K_{i\,app})^2 - 4[E][I]}}{2[E]} \quad (1)$$

where v is the reaction velocity at different concentrations of inhibitor I, v_0 is the control velocity in the absence of inhibitor, and [E] is the total enzyme concentration.

Inhibitor modality (e.g., competitive, noncompetitive, uncompetitive, or mixed) under steady-state conditions was determined by measuring the effect of inhibitor concentration on initial velocity as a function of substrate concentrations. Data were fit using equations in GraFit (version 5.0.11; Erithiacus Software Ltd.) to velocity equations for the various modes of inhibition.

Determination of the Residence Half-Life ($t_{1/2}$) for Ispinesib. The residence half-life ($t_{1/2}$) for *ispinesib* dissociation from KSP was determined by equilibrium dialysis. Measurements were performed in a final reaction volume of 1 mL consisting of 800 nM KSP, 800 nM *ispinesib*, and 5 μM MT. The solution was loaded into dialysis cassettes and dialyzed against PEM25 buffer supplemented with 2 mM DTT for 30 h. The dialysis buffer was changed three times during the first 2 h to ensure complete dialysis. Aliquots of reaction samples were collected at various time points and tested for activity. The activities of the reaction samples were normalized to the activities of a DMSO (no inhibitor) control.

Table 1: Comparison of Kinetic Constants for KSP−MT ATPase ± *Ispinesib*

constants		no inhibitor (control)	*ispinesib*
steady-state ATPase	k_{cat} (s^{-1})	9.3 ± 0.7	
	$K_{m,ATP}$ (μM)	21 ± 1.1	
	$K_{m,MT}$ (μM)	0.85 ± 0.05	
	$K_{i\ app,ispinesib}$ (nM)		1.7 ± 0.1
steady-state mechanism of inhibition of *ispinesib*			ATP uncompetitive ($K_{i\ app}$ = 3.1 ± 0.2 nM)
			MT competitive-like ($K_{i\ app}$ = 3.7 ± 0.2 nM, α = 8 ± 0.3)
ispinesib dissociation[a]	$t_{1/2}$ (s^{-1})		$<5 \times 10^{-6}$
	k_{off} (h)		>40
ispinesib association[b]	$k_{on,KSP\cdot ADP}$ ($\mu M\ s^{-1}$)		9.4 ± 0.2
	$k_{on,KSP\cdot AMPPNP}$ ($\mu M\ s^{-1}$)		10.6 ± 0.7
	$k_{on,KSP-MT\ (rigor)}$ ($\mu M\ s^{-1}$)		2.1 ± 0.3
	$k_{on,KSP\cdot AMPPNP-MT}$ ($\mu M\ s^{-1}$)		1.9 ± 0.1
microtubule association[c]	$k_{on,KSP-MT\ (rigor)}$ ($\mu M\ s^{-1}$)	9.7 ± 0.7	
	$k_{on,KSP\cdot AMPPNP-MT}$ ($\mu M\ s^{-1}$)	13.2 ± 0.9	
ATP-promoted MT dissociation[c]	k_{max} (s^{-1})	7.2 ± 0.2	42.3 ± 2.7
	$K_{1/2,ATP}$ (μM)	15 ± 2	4 ± 0.3
mantATP binding	k_{on} ($\mu M\ s^{-1}$)	2.8 ± 0.09	3.7 ± 0.09
	k_{off} (s^{-1})	16.1 ± 0.9	11.6 ± 0.8
phosphate release[d]	k_{max} (s^{-1})	9.5 ± 0.5	39 ± 0.7
	$K_{1/2,ATP}$ (μM)	5.1 ± 0.5	11.8 ± 0.8
mantADP release (with MTs)[e]	k_{max} (s^{-1})	72 ± 3.5	
	$K_{1/2,ATP}$ (μM)	7.1 ± 0.8	
	$k_{off,mantADP}$ ($\mu M\ s^{-1}$)	4.2 ± 0.7[f]	0.014 ± 0.007[f]
mantADP release (no MTs)[e]	$k_{off,mantADP}$ (s^{-1})	0.11 ± 0.08	0.0052 ± 0.0002

[a] Determined by equilibrium dialysis. [b] Determined using Trp fluorescence. [c] Determined using turbidity (*21*). [d] Determined using the fluorescent phosphate reporter MDCC-PBP (*22*). [e] Determined by competing mantADP with excess unlabeled MgATP (*21*). [f] Fitted to a linear equation between 0 and 16 μM MTs.

The release rates (k_{off}) for *ispinesib* were determined by single-exponential fitting of the experimental data. The residence half-life ($t_{1/2}$) was calculated using eq 2.

$$t_{1/2} = 0.693/k_{off} \quad (2)$$

Transient-State Experiments. Stopped-flow (SF-61 DX2; Hi-Tech Scientific) experiments were conducted to determine the effect of *ispinesib* on mantATP binding, KSP association and disassociation from MTs, phosphate (P_i) release, and mantADP release. A nucleotide-free KSP−MT complex was prepared by incubating a 1:1 complex of KSP and MT with 1 unit/mL apyrase for 15 min at room temperature. Apyrase was removed through a 20% sucrose cushion by centrifugation (75000*g*) for 15 min. The pelleted KSP−MT complex was resuspended in PEM25 buffer supplemented with 10 μM paclitaxel.

For each data point transient traces were collected in triplicate and averaged, before fitting. For mantATP or mantADP experiments, fluorescence emission was measured using a 400 nm cutoff filter with excitation at 360 nm. The increase in fluorescence upon KSP binding to mantATP or decrease in fluorescence following the release of mantADP from KSP was monitored as previously described (*21*). The rates of P_i release were measured using the bacterial phosphate binding protein (PBP) modified with 7-diethylamino-3-[[[2-(maleimidyl)ethyl]amino]carbonyl]coumarin (MDCC) dye (*21, 22*). The nucleotide-free KSP−MT complex plus MDCC-PBP and P_i-mop (vide infra) was rapidly mixed with increasing concentrations of MgATP and P_i-mop. The P_i-mop consisted of a solution of PNPase (10 units/mL), 7-MEG (10 mM), $MnCl_2$ (5 μM), glucose 1,6-bisphosphate (1 mM), and PDRM (1 μg/mL) in a ratio to eliminate competition with MDCC-PBP for P_i in solution. KSP−MT complex dissociation and association kinetics were monitored by the change in solution turbidity at 340 nm (*21*). Experiments measuring KSP dissociation rates from MTs were conducted using MgATP as previously described (*21, 23*). Briefly, a complex of nucleotide-free KSP and microtubules was preformed in the absence and presence of *ispinesib* and rapidly mixed in the stopped-flow instrument with varying concentrations of MgATP (0–500 μM) and KCl (100 mM) in PEM25. In this experimental design, KSP binds and hydrolyzes ATP, which results in the detachment of KSP from the microtubule. The additional salt (KCl) weakens the interaction of the motor with MT, minimizing MT rebinding.

To determine the binding rate of *ispinesib* to KSP, we monitored Trp127 fluorescence. The rates of *ispinesib* binding to KSP under its various physiological states (KSP−MT, KSP−AMPPMP−MT (ATP-like), KSP−ADP, and KSP−AMPPNP) were determined by monitoring fluorescence quenching of Trp127 within the loop 5 region (*16*). The excitation wavelength was 295 nm, and the emission filter cutoff was 320 nm. The stock solutions of *ispinesib* (0–100 μM) and KSP or KSP−MT (1 μM) in the presence of either 500 μM ADP or 500 μM AMP-PNP in PEM25 buffer were mixed by a stopped-flow apparatus. The fluorescence quenching traces were fitted to a double-exponential equation.

RESULTS

Ispinesib Is a Potent, Specific Inhibitor of KSP. The construct we used for our studies was a truncated KSP motor domain, KSP360, encoding for the initial 360 amino acids of the core KSP motor domain and a portion of the neck linker with a carboxy-terminal hexahistidine tag. This relatively compact domain is the defining structural feature of a kinesin as it is responsible for ATP hydrolysis and generation of motile force along the microtubules (*24, 25*). We screened a collection of small synthetic organic com-

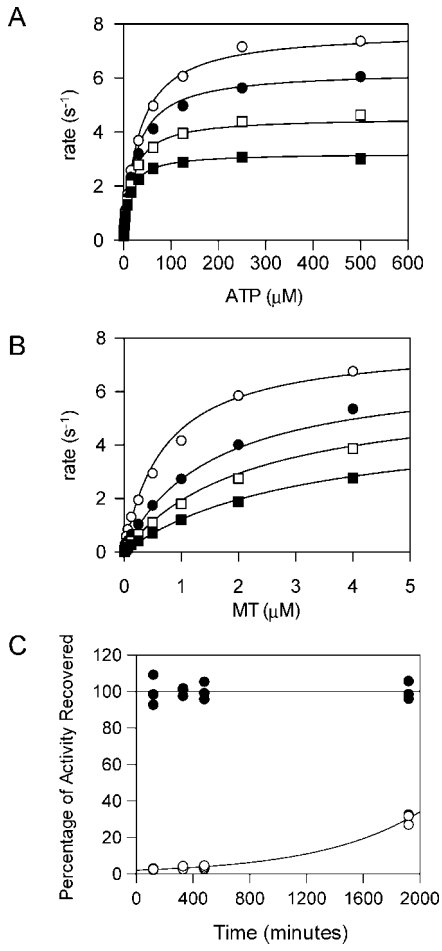

FIGURE 2: Mode of inhibition studies of *ispinesib* by varying (A) the ATP concentration in the presence of saturating MT with 4 nM *ispinesib* (■), 2 nM *ispinesib* (□), 1 nM *ispinesib* (●), and 0 nM *ispinesib* (○) and (B) the MT concentration in the presence of saturating ATP with 4 nM *ispinesib* (■), 2 nM *ispinesib* (□), 1 nM *ispinesib* (●), and 0 nM *ispinesib* (○). The KSP concentration in these reactions was 0.75 nM. (C) Recovery of KSP activity from *ispinesib* (○) following dialysis. Data was normalized to the "no inhibitor control" (●), and the resulting experimental data were fitted to a single exponential. In this reaction the concentration of KSP was 800 nM, MT was 5 μM, and *ispinesib* was 800 nM.

pounds for inhibitors of the KSP motor domain activity and identified a series of quinazolinone inhibitors. Synthetic chemical optimization improved the biochemical, cellular, and drug-like properties of these compounds, finally leading to the identification of *ispinesib* (Figure 1A) (*26, 27*).

ATP-turnover kinetics under steady-state conditions revealed that our purified KSP protein was active. In the presence of MT, the maximum KSP activity was 9.3 ± 0.7 s^{-1}, agreeing with previous reports (*9, 11, 16, 23*). The K_m values for ATP and MT were 21 ± 1.1 μM and 0.85 ± 0.05 μM (Table 1), respectively, which again is consistent with previously reported values (*9, 11, 16, 23*). Concentration–response studies of *ispinesib* inhibition of KSP revealed that *ispinesib* was a potent inhibitor of the MT-stimulated ATPase activity (Figure 1B) with $K_{i\,app}$ = 1.7 ± 0.1 nM. Importantly, the activity of *ispinesib* was highly specific for KSP (Figure 1C). At 20 μM inhibitor concentration, more than 10000-fold the K_i for KSP, no inhibitory activity was observed toward the mitotic kinesins CENP-E, RabK6, MCAK, and MKLP1, the ubiquitous kinesin heavy chain (KHC), or toward the neuronal kinesin Kif1A.

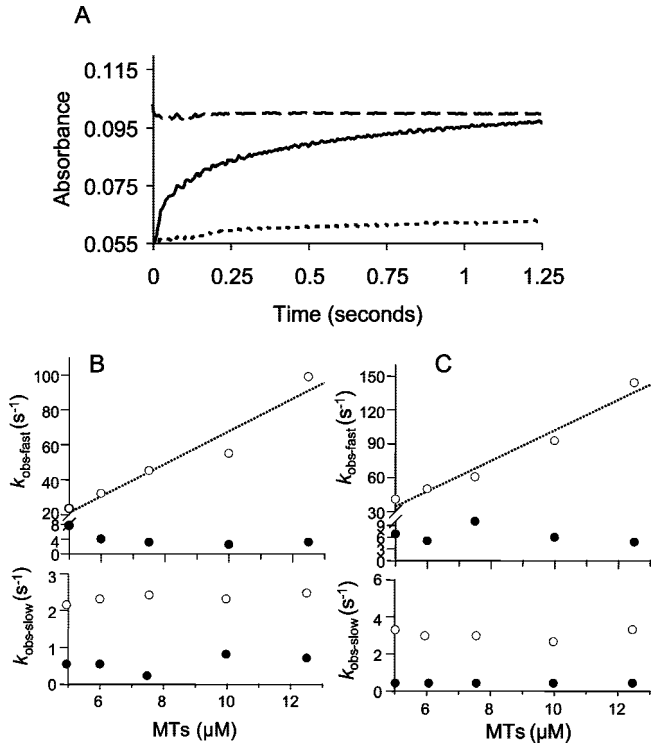

FIGURE 3: Kinetics of KSP association with MT ± *ispinesib*. (A) Representative stopped-flow transient traces for 5 μM KSP ± *ispinesib* rapidly mixed with 5 μM MT (solid black line for 0 μM inhibitor and black dotted line for 20 μM *ispinesib*) and a preformed KSP−MT complex (5 μM) rapidly mixed with buffer (black dashed line). (B) Rate constants for the rate of KSP−MT complex formation in the nucleotide-free state plotted as a function of MT concentration in the absence (○ with dotted line) and presence of 20 μM *ispinesib* (● with solid line). (C) Rate constants for the rate of KSP-MT complex formation in the ATP-like (AMP-PNP) state plotted as a function of MT concentration in the absence (○ with dotted line) and presence of 20 μM *ispinesib* (● with solid line). Stopped-flow transient traces were fitted to a double-exponential equation in order to determine the fast and slow association processes [top and bottom panels, respectively, for (B) and (C)]. The fast phase experimental rates ($k_{obs,fast}$) in the absence of *ispinesib* were fitted to a linear equation in order to determine the second-order rate constant.

Ispinesib Is an Allosteric, Reversible Inhibitor of KSP. We initially studied the mode of inhibition of *ispinesib* by steady-state kinetic analysis of MT-stimulated ATP hydrolysis in the presence of varying concentrations of ATP (Figure 2A). The plot shows that *ispinesib* is an ATP uncompetitive inhibitor with an apparent inhibition constant ($K_{i\,app}$) of 3.1 ± 0.2 nM. Studies with varying concentrations of MTs and *ispinesib* in the presence of a saturating concentration of ATP reveal that *ispinesib* acts via a mixed competitive-like mechanism with respect to MT (Figure 2B) with a $K_{i\,app}$ = 3.7 ± 0.2 nM and $\alpha = 8 \pm 0.3$ ($\alpha = K_i'/K_i$, ratio of inhibitor binding constants to enzyme–substrate complex vs free enzyme).

The dissociation rate of *ispinesib* from KSP (k_{off}) was estimated to be less than 5×10^{-6} s^{-1} using equilibrium dialysis, corresponding to a residence half-life ($t_{1/2}$) longer than 40 h. Furthermore, the recovery of KSP enzymatic activity upon dialysis suggests that *ispinesib* is a slow reversible inhibitor of KSP (Figure 2C).

Ispinesib Slows the Association of KSP to MT. We further examined the interaction of KSP with MT under two states [nucleotide-free and AMPPNP (ATP-like) state] in the

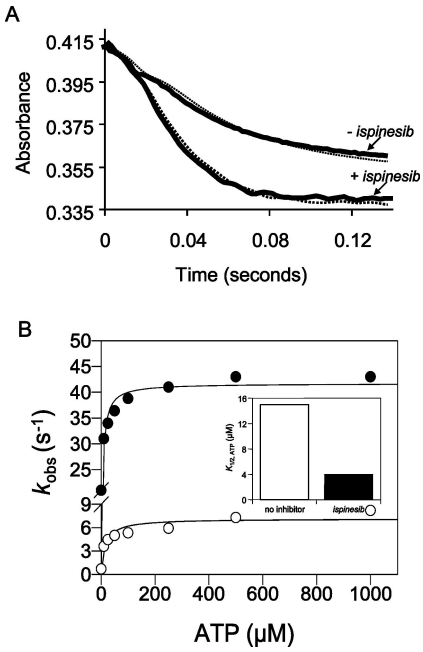

FIGURE 4: Kinetics of ATP-promoted dissociation of the KSP−MT complex ± *ispinesib*. A preformed KSP−MT complex (5 μM) ± *ispinesib* (20 μM) was rapidly mixed in the stopped-flow instrument with varying concentrations of MgATP plus KCl (100 mM). (A) Representative stopped-flow transient traces for reaction in the absence and presence of *ispinesib* rapidly mixed with 10 μM MgATP. Transient traces were satisfactorily fitted to a single-exponential process (gray dotted line). (B) The rate of the dissociation process plotted as a function of MgATP concentration in the absence (○) and presence of *ispinesib* (●). Experimental data were fitted to a hyperbolic curve in order to determine a maximum rate. Inset: Bar chart comparing the $K_{1/2,ATP}$ for ATP-promoted dissociation of the KSP−MT complex ± *ispinesib*.

presence and absence of *ispinesib* by monitoring the turbidimetric changes as KSP associated with MTs. Using a stopped-flow instrument, we rapidly mixed KSP with and without *ispinesib* (20 μM) with varied MT concentrations. In both nucleotide states we observed biphasic transient traces for the formation of the KSP−MT complex (Figure 3A). In each experiment we found that the total change in absorbance for all biphasic traces was close to the theoretical maximum absorbance (determined by monitoring the absorbance change of a preformed KSP−MT complex; Figure 3A). In both nucleotide states of KSP the observed rates for the fast phase ($k_{obs,fast}$) were linearly dependent on MT concentration without approaching saturation at any accessible MT concentration (Figure 3B,C). The second-order rate constant calculated from the slope of the plots was 9.7 ± 0.7 μM^{-1} s^{-1} and 13.2 ± 0.9 μM^{-1} s^{-1} for the nucleotide-free and ATP-like state, respectively. However, the observed rates for the slow phase ($k_{obs,slow}$) were independent of MT concentration. We believe the initial fast phase of this biphasic process represents the association of KSP to MTs whereas the slower phase most likely represents a conformation change in the newly formed KSP−MT complex. In Figure 3A we show representative transient traces for the association of KSP to MT with and without *ispinesib* (20 μM). We found that the observed amplitude change, which represents the formation of the KSP−MT complex, is diminished in the presence of a fixed concentration of *ispinesib*, indicating that *ispinesib* inhibits the association of KSP with MT. In both nucleotide states of KSP the observed rates for the fast phase ($k_{obs,fast}$) are dramatically reduced in the presence of *ispinesib* (Figure 3B,C). These data are consistent with our steady-state experiments, which also showed that *ispinesib* weakens the interaction of KSP with MT during ATP turnover (Table 1).

Ispinesib Accelerates ATP-Promoted Dissociation of KSP from MT. Using the stopped-flow a preformed KSP−MT (5 μM) complex with and without *ispinesib* was rapidly mixed with increasing concentrations of MgATP. In this experimental configuration KSP binds and hydrolyzes ATP, which is followed by detachment of the motor from MT. Figure 4A shows representative traces in the absence and presence of *ispinesib* (20 μM) at a fixed concentration of MgATP (10 μM). The dissociation kinetics shows a saturable ATP concentration dependence (Figure 4B) with a maximum rate of KSP−MT dissociation of 7.2 ± 0.2 s^{-1} which is almost identical to that previously reported (*23, 28*). In the presence of a fixed concentration of *ispinesib* (20 μM), we observe an approximate 4-fold increase in the maximum rate of KSP−MT dissociation (42.3 ± 2.7 s^{-1}), indicating that *ispinesib* accelerates ATP-promoted dissociation of KSP from MT by destabilizing the KSP−MT complex (Figure 4 and Table 1). Interestingly, in the presence of *ispinesib* the $K_{1/2,ATP}$ value dropped by ~3-fold from 15 ± 2 μM to 4 ± 0.3 μM (Figure 4B, inset).

Binding of Ispinesib Is Slowed in the Presence of MT. Ispinesib binds to an induced-fit pocket, situated between helix α3 and loop L5 of helix α2 (*29*). Surprisingly, the *ispinesib* binding site occupies an almost identical location to that identified for monastrol (*13*), despite the absence of any obvious structural similarity between the two compounds. Upon binding of either *ispinesib* or monastrol, the loop L5 moves downward ~7 Å, and the side chain of Trp127, which is located at the tip of loop L5, moves ~10 Å to cap the entrance of the newly formed pocket. Since Trp127 is the only tryptophan residue in our KSP motor domain construct, the fluorescence signal from Trp127 serves as a probe to detect the binding of *ispinesib* to KSP. This spectroscopic strategy has been used in prior studies that demonstrated mixing KSP in the ADP state with monastrol quenched the tryptophan fluorescence emission in a monophasic kinetic process (*16, 30*). Like monastrol, we also observed the fluorescence quenching upon addition of *ispinesib* to a KSP solution (Figure 5A). In this experiment the fluorescence spectra of 1 μM KSP solutions were recorded, as the average of a 1 min reading, before and after the addition of *ispinesib* (10 μM). In the presence of MT, the fluorescence quenching upon addition of *ispinesib* was also observed; however, the amplitude of quenching was attenuated (Figure 5B).

The fluorescence quenching of Trp127 was further utilized to determine the pre-equilibrium binding rate of *ispinesib* to KSP in various states. The rate of *ispinesib* binding to KSP was monitored by rapid mixing of KSP or a KSP−MT complex (1 μM) and various concentrations of *ispinesib* (10−100 μM). Interestingly, the resulting transient traces from the reaction were biphasic in each state (Figure 5C,D). A closer look at the fitting showed that only the fast phase was *ispinesib* concentration dependent (Figure 5E). The slow phase was not dependent on *ispinesib* concentration and more than 1 magnitude slower than the fast phase (Figure 5F). The relative amplitudes of the fast phase were ~80% and ~88% of the total amplitude change in the absence and

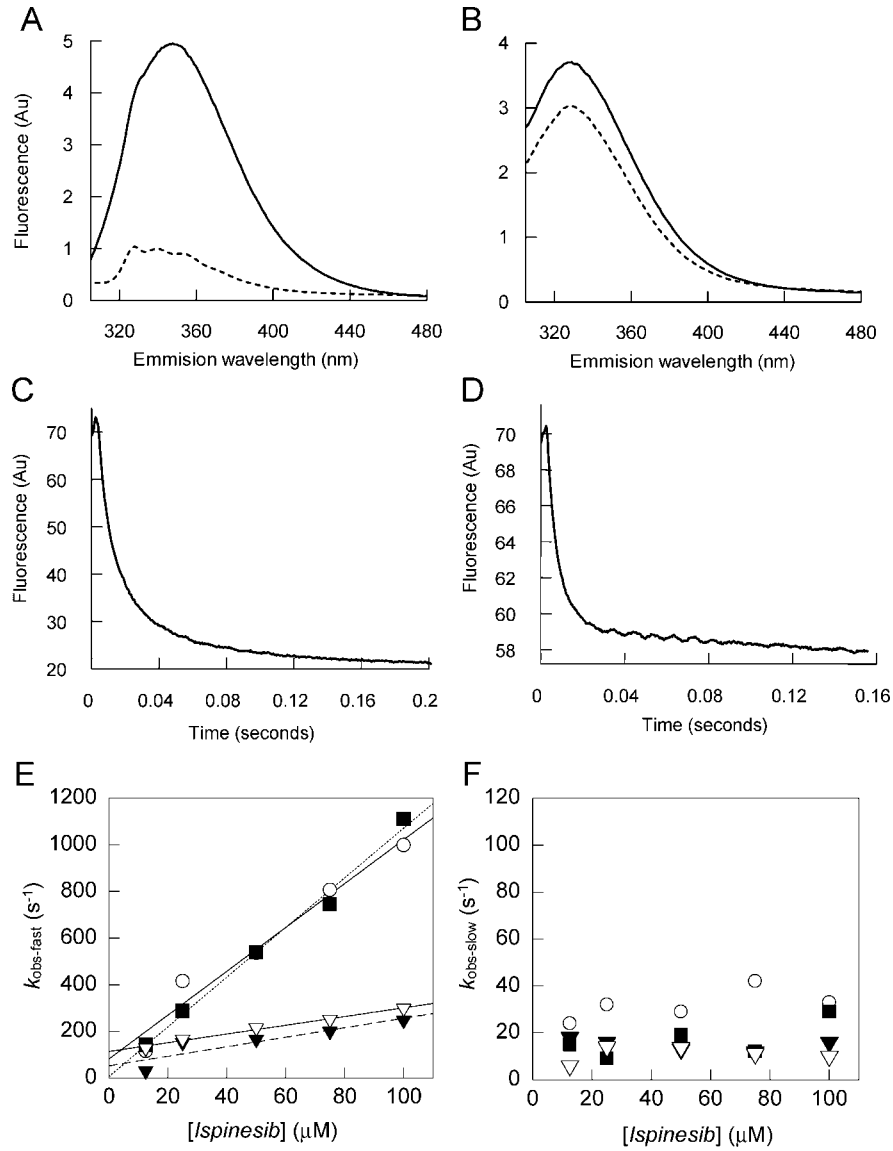

FIGURE 5: (A) Fluorescence emission spectra of 1 μM KSP (nucleotide-free) in the absence (solid line) and presence of 10 μM *ispinesib* (dashed line) taken in PEM25 buffer at 25 °C. (B) Fluorescence emission spectra of 1 μM KSP−MT complex in the absence (solid line) and presence of 10 μM *ispinesib* (dashed line) taken in PEM25 buffer at 25 °C. (C) Biphasic stopped-flow transient trace obtained after mixing 1 μM KSP (nucleotide-free) and 10 μM *ispinesib*. (D) Biphasic stopped-flow transient trace obtained after mixing 1 μM KSP−MT and 10 μM *ispinesib*. (E, F) Binding rate constants for fast (left) and slow (right) processes of *ispinesib* binding to the KSP−ADP (○), KSP−AMPPNP (■), KSP−MT (▼) and KSP−AMPPNP−MT (▽). The data for the fast phase ($k_{obs,fast}$) were fitted to a linear equation.

presence of MT, respectively, and did not change as a function of *ispinesib* concentration. The relative amplitudes of the slow phase were ~20% and ~12% of the total amplitude change in the absence and presence of MT, respectively, and likely reflect a conformational change subsequent to *ispinesib* binding. The second-order k_{on} rate constants obtained from the slopes of the fast-phase plots (Figure 5E) are shown in Table 1. We found that the rate constant for *ispinesib* binding to KSP in the presence of MT was approximately 5-fold slower than binding to the basal form of the motor. These results suggest that *ispinesib* has a higher affinity for the basal form of the motor than the MT complex. This is consistent with our earlier data (steady state and pre steady state) where we showed that *ispinesib* is MT-competitive and that *ispinesib* blocks the association of KSP to MT. Unlike monastrol, which appears to exhibit better binding to KSP in the presence of ADP than the KSP−AMP-PNP complex (*16*), *ispinesib* does not show such a preference.

Ispinesib Inhibits ADP Release with and without MT. KSP (2.5 μM) was incubated with mantADP to exchange any nucleotide at the active site with mantADP. The resulting complex was incubated with and without *ispinesib* (20 μM) and rapidly mixed with an excess of MgATP (1 mM) and increasing concentrations of MT (0–40 μM). The excess of MgATP prevents rebinding of mantADP to the KSP complex. Figure 6A shows representative transient traces for mantADP release in the absence of MT with and without *ispinesib*. The mantADP release rate from the KSP−mantADP complex in the absence of MT was 0.11 ± 0.08 s^{-1} and is comparable to the rate previously reported for KSP (*28*). In the presence of *ispinesib* we observe a dramatic slowing of mantADP release (Figure 6A, Table 1). *Ispinesib* decreased the mantADP release rate more than 20-fold, from 0.11 s^{-1}

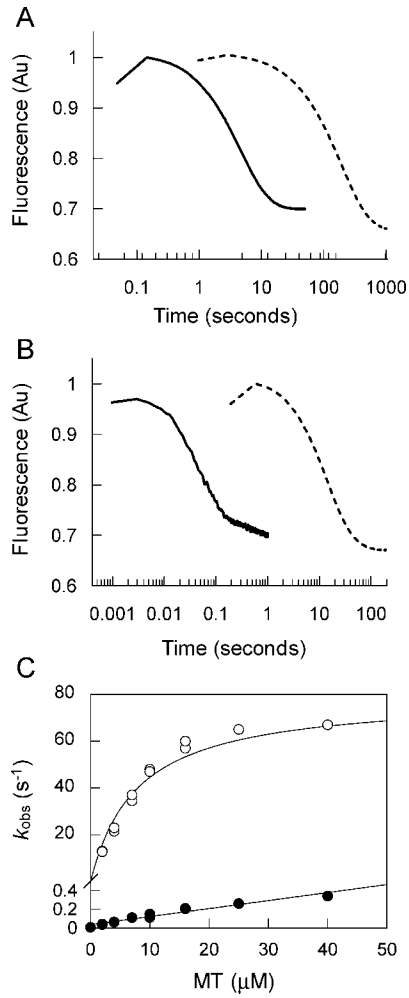

FIGURE 6: Effect of *ispinesib* on mantADP release from KSP. (A) Stopped-flow transient traces showing the slowing of mantADP release in the absence of MT by *ispinesib* (dotted line) compared to the no inhibitor trace (solid line). Conditions were 2.5 μM KSP−mantADP, 20 μM *ispinesib*, and 1 mM MgATP. (B) Transient stopped-flow traces showing the slowing of MT-stimulated mantADP release by 20 μM *ispinesib* (dotted line) compared to the no inhibitor trace (solid line). Final concentrations were 2.5 μM KSP−mantADP, 20 μM *ispinesib*, and 1 mM MgATP. (C) The rate constants (k_{obs}) obtained from a single-exponential fit of the experimental data were plotted as a function of MT concentration in the absence (○) and presence of *ispinesib* (●). The second-order rate constants for MT-stimulated release were determined by a fit of the data to the initial linear phase (0–16 μM MT). In the absence of *ispinesib* experimental data were fitted to a hyperbolic curve in order to determine a maximum rate.

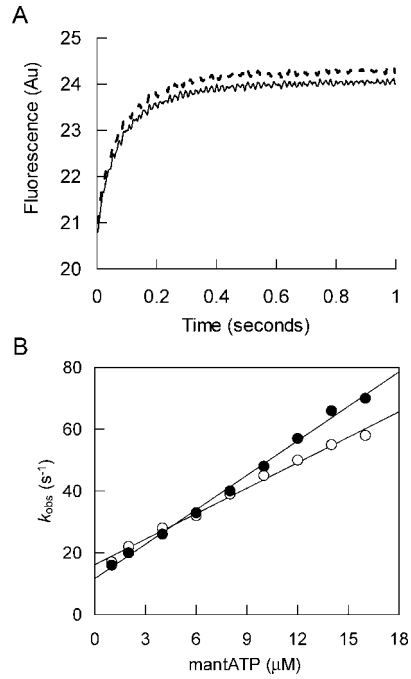

FIGURE 7: Effect of *ispinesib* on mantATP to the KSP−MT complex. (A) Stopped-flow transient traces showing that mantATP (4 μM) binding to the KSP−MT (3 μM) complex is unaffected by *ispinesib* (dotted line) compared to the no inhibitor trace (solid line). (B) The rate constants (k_{obs}) obtained from a single-exponential fit of the experimental data were plotted as a function of mantATP concentration in the absence (○) and presence of *ispinesib* (●). The second-order rate constants for MT-stimulated release were determined from the slopes of the plot. Final concentrations were 20 μM *ispinesib*, 0.5 μM KSP−MT for 1–2 μM mantATP, and 3 μM KSP−MT for 4–16 μM mantATP.

to 0.0052 ± 0.0002 s^{-1}. In the presence of increasing MT concentrations we also observed a dramatic slowing of mantADP release in the presence of a fixed concentration of *ispinesib* (Figure 6B,C). The dissociation of mantADP in the absence of *ispinesib* showed a saturable MT concentration dependence (Figure 6C) with a maximum rate of 72 ± 3.5 s^{-1} and a $K_{1/2,MT}$ of 7.1 ± 0.8 μM (Table 1), which is approximately 2-fold higher than previously reported (*23*). In the presence of *ispinesib* the release rate of mantADP was linearly dependent on MT concentration without approaching saturation at any accessible MT concentration. A fit of the data to the initial linear phase of Figure 6C (0–16 μM MT) yields a second-order rate constant and showed that *ispinesib* decreased the rate of mantADP release by ~300-fold, from 4.1 ± 0.2 μM^{-1} s^{-1} to 0.014 ± 0.007 μM^{-1} s^{-1}.

These results suggest that *ispinesib* stabilizes the KSP−mantADP complex in the presence and absence of MT.

Ispinesib Does Not Perturb mantATP Binding to the KSP−MT Complex. Our steady-state data and the crystal structure of the KSP−*ispinesib* complex (*29*) suggest that *ispinesib* is not competitive with respect to MgATP. To determine whether the pre-steady-state step of ATP binding to the KSP−MT complex was perturbed, we rapidly mixed a preformed complex of KSP−MT (0.5–3 μM) with and without *ispinesib* (20 μM) with varied concentrations of mantATP (1–16 μM). The observed rates (k_{obs}) for the formation of the KSP−mantATP complex showed a linear dependence on mantATP concentration between 1 and 16 μM (Figure 7). In the absence of *ispinesib* the second-order rate constant for mantATP binding was found to be 2.8 ± 0.09 μM^{-1} s^{-1} and a mantATP dissociation rate of 16.1 s^{-1} (Table 1) which is comparable to that previously reported (*23*). In the presence of a fixed concentration of *ispinesib* (20 μM) the rates of mantATP binding and mantATP dissociation were found to be only modestly affected when compared to the no inhibitor rate constants (3.7 ± 0.09 μM^{-1} s^{-1} and k_{off} = 11.6 s^{-1}), suggesting that binding of nucleotide is not strongly perturbed by *ispinesib* treatment.

Ispinesib Accelerates Phosphate Release from the KSP−MT Complex. ATP binding and hydrolysis by KSP is followed by the release of P_i from the ADP·P_i state. We measured the kinetics of P_i release using the fluorescent phosphate reporter MDCC-PBP (*22*). For this assay a KSP−MT complex (2 μM KSP and 10 μM MT, pretreated with apyrase

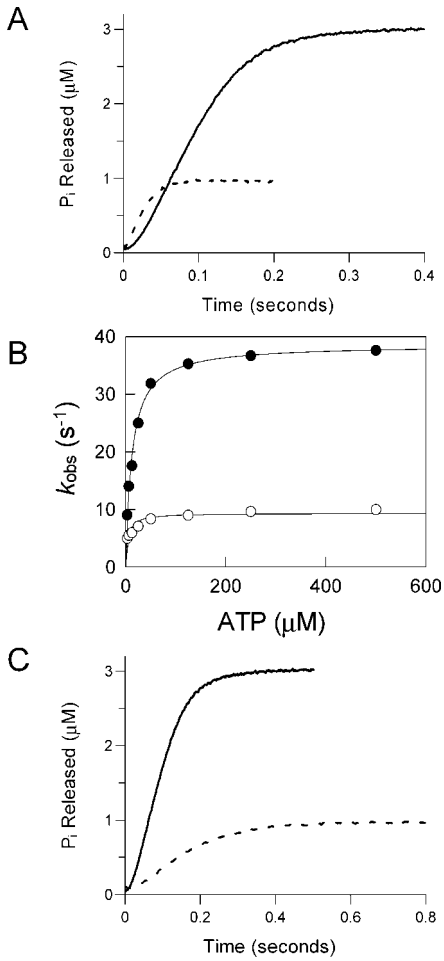

FIGURE 8: Kinetics of phosphate release from the KSP−MT complex ± *ispinesib*. (A) Stopped-flow transient traces showing the fluorescent enhancement of MDCC-PBP upon binding of inorganic phosphate (P_i) released from a KSP−MT no inhibitor complex (solid line) and a KSP−MT−*ispinesib* complex (dotted line). Final concentrations: 1 μM KSP, 4 μM MT, 250 μM ATP, 20 μM *ispinesib*, 8 μM MDCC-PBP, 10 units/mL PNPase, 10 mM 7-MEG, 5 μM $MnCl_2$, 1 mM glucose 1,6-bisphosphate, 1 μg/mL PDRM in PEM25. (B) The rate constants (k_{obs}) obtained from a single-exponential fit of the experimental data were plotted as a function of MgATP concentration in the absence (○) and presence of *ispinesib* (●). The first-order rate constants for P_i release of the experimental data were fitted to a hyperbolic curve in order to determine a maximum rate. (C) Stopped-flow transient traces showing the release of inorganic phosphate (P_i) from a KSP−MT complex in the absence of high salt (solid line) and presence of 400 mM KCl (dotted line). Final concentrations: 1 μM KSP, 4 μM MT, 250 μM ATP, 8 μM MDCC-PBP, 10 units/mL PNPase, 10 mM 7-MEG, 5 μM $MnCl_2$, 1 mM glucose 1,6-bisphosphate, 1 μg/mL PDRM in PEM25, and ±400 mM KCl.

to remove any residual ADP), with and without *ispinesib* (20 μM), and MDCC-PBP (8 μM) were rapidly mixed with varying concentrations of MgATP. When inorganic phosphate is released from the active site of KSP, the phosphate binding protein binds the free P_i rapidly and tightly, giving rise to an approximate 5-fold increase in fluorescence intensity (*21, 22*). The observed amplitude of the kinetic traces was converted to P_i concentration (micromolar) based on a control experiment in which MDCC-PBP was rapidly mixed with known concentrations of sodium phosphate. In the absence of the inhibitor we observed continued product formation without evidence of burst kinetics (Figure 8A). The kinetics of P_i release shows an ATP concentration

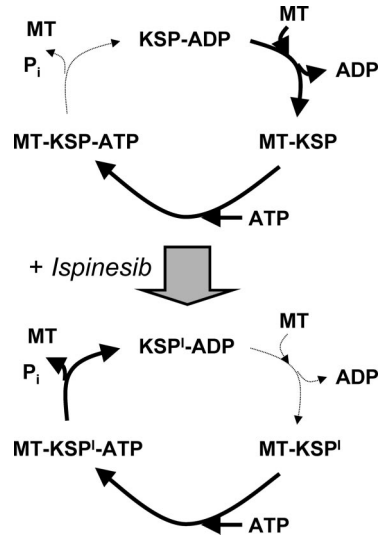

FIGURE 9: Proposed kinetic model summarizing the biochemical mechanism of action of *ispinesib*. The model illustrates that in the absence of *ispinesib* (top figure) the rate-limiting step of the MT-stimulated KSP ATPase cycle is P_i release coupled with KSP detachment from MT (dotted arrows). In the presence of *ispinesib* (bottom panel) KSP is locked in the ADP state with a compromised ability to bind MT. The kinetic steps leading to the ADP state (P_i release, MT release) are accelerated, while steps leading away from the ADP state (ADP release) are dramatically inhibited (dotted arrows).

dependence with a maximum P_i release rate of 9.5 ± 0.5 s^{-1} and a $K_{1/2,ATP}$ of 5.1 ± 0.5 μM (Figure 8B, Table 1) and is consistent with previously reported values (*28*). The maximum rate of P_i release is almost identical to the maximum steady-state turnover rate (k_{cat} = 9.3 s^{-1}) and comparable to the observed rate of ATP-promoted dissociation of the KSP−MT complex (7.2 s^{-1}, Table 1). These results suggest that the rate-limiting step in the KSP catalytic cycle corresponds to P_i release coupled with KSP detachment from MT and is consistent with the kinetics reported from another KSP enzymatic characterization study (*28*). In the presence of *ispinesib*, the rate of P_i release is significantly accelerated but the amplitude is reduced to a value consistent with a single enzymatic turnover (Figure 8A). This reduction in P_i release amplitude is consistent with dramatic*ispinesib*-induced inhibition of subsequent enzymatic steps, mainly ADP release. A similar change in amplitude can be induced in the absence of *ispinesib* by mixing the KSP−MT complex with ATP under high ionic strength conditions (400 mM KCl; Figure 8C). High ionic strength prevents KSP−ADP rebinding to MTs, which results in a single-turnover conditions. It is noteworthy that the observed rate of P_i release in 400 mM KCl is not significantly changed compared to the low ionic strength rate. The observed increase in P_i release rates in the presence of *ispinesib* shows an ATP concentration dependence. The maximum rate of P_i release is increased from 9.5 ± 0.5 s^{-1} to 39 ± 0.7 s^{-1} whereas the $K_{1/2,ATP}$ changes from 5.1 ± 0.5 μM to 11.8 ± 0.8 μM in the presence of the inhibitor (Figure 8B).

DISCUSSION

In this present study we have used steady-state and pre-steady-state methodologies to define the molecular basis for KSP inhibition by *ispinesib*. Our results show that *ispinesib*

is a highly specific, potent inhibitor of the KSP ATPase. The steady-state kinetic measurements reveal that *ispinesib* is an ATP-uncompetitive and MT-competitive inhibitor. These data are consistent with the crystallographic data which have shown *ispinesib* binding to a site that is ~12 Å away from the nucleotide binding pocket. *Ispinesib* binding is accompanied by a large structural change in the switch I and switch II regions of KSP (*29*). These regions are reported to be important for MT binding (*31*), providing a plausible mechanism by which binding of this inhibitor causes a structural reorganization of KSP that weakens MT association without direct inhibitor binding to the KSP−MT interface. KSP−MT binding experiments further support the MT-competitive nature of *ispinesib*. Turbidity experiments monitoring the association kinetics between KSP and MT reveal that *ispinesib* essentially prevents the formation of a KSP−MT complex, whereas the ATP-promoted dissociation kinetics of KSP from MT show that *ispinesib* accelerates this step. This provides further evidence that *ispinesib* disfavors the formation of a KSP−MT complex and prefers binding to the basal form of the enzyme. *Ispinesib*'s preference for the basal form of the motor rather than the KSP−MT is reinforced by direct inhibitor binding experiments. Pre-equilibrium binding data reveal that *ispinesib* binds approximately 5-fold faster to the basal form of KSP than to a KSP−MT complex. Surprisingly, although *ispinesib* shows a preference for KSP alone rather than the KSP−MT complex, it does not differentiate between various nucleotide states (Table 1). In this respect, *ispinesib* is distinct from monastrol, which in similar preequilibrium binding experiments bound faster to KSP in the ADP than the AMP-PNP (ATP-like) state (*16*).

Our mantADP release experiments show that *ispinesib* slows the release of mantADP in the absence and presence of MT in a fashion similar to monastrol (*17, 18*), indicating that both compounds stabilize KSP in the ADP nucleotide state. When we further compare the steady-state and pre-steady-state mode of inhibition data between *ispinesib* and monastrol, we find that both inhibitors affect KSP in a similar manner. Like *ispinesib*, the steady-state mode of KSP inhibition by monastrol is ATP-uncompetitive (*11, 17*) and MT-mixed competitive. The MT-competitive nature of monastrol is supported further by equilibrium binding studies and pre-steady-state MT association kinetics which showed that monastrol inhibits the association of KSP to MT (*17*). However, in the same study, the most intriguing data reported for monastrol were its effect on the rate of ATP hydrolysis. A detailed quench-flow study revealed that monastrol increased the pre-steady-state burst kinetics of ATP hydrolysis from the KSP−MT complex. Interestingly, the increase in the burst rate was accompanied by a concomitant decrease in the burst amplitude (*17*). This decreased burst amplitude and increased burst rate were interpreted as reversal of ATP hydrolysis, and it was proposed that monastrol stabilizes the KSP ATP hydrolysis conformation such that ATP resynthesis becomes energetically favorable. If the reversal of the ATP hydrolysis step in the presence of monastrol occurred, then one would expect monastrol to inhibit P_i release from the KSP motor domain after ATP hydrolysis. In our study for the mechanistic characterization of *ispinesib* we have not directly examined the effect of *ispinesib* on the rate of ATP hydrolysis, but we have measured the inhibitor effect on P_i release. Our experiments reveal that *ispinesib* significantly accelerates the rate of P_i release and that the amount of P_i released approximates the concentration of the KSP motor domain. This observation is inconsistent with a significant degree of ATP resynthesis in the presence of *ispinesib*.

In summary, our results show that the primary mode of inhibition by *ispinesib* is to lock the motor in the ADP state with a compromised ability to bind MT (Figure 9). Kinetic steps leading to the ADP state (P_i release, MT release) are accelerated, while steps leading away from the ADP state (ADP release) are dramatically inhibited. When compared to monastrol, we find that both inhibitors have a similar mechanism of action, with a possible exception for the effect on ATP resynthesis. The data presented in this study suggest that targeting the loop L5 binding pocket on KSP with a small-molecule inhibitor leads to a common mechanism of action. Identifying novel, potent, small-molecule, allosteric inhibitors that bind KSP at sites distinct from loop L5 may result in a different mechanism of KSP inhibition, perhaps with a different spectrum of *in vivo* activity.

ACKNOWLEDGMENT

Yan Lee and Kim Suekawa are gratefully acknowledged for protein preparations. We thank Dr. Hector Rodriguez, Dr. Katjusa Brejc, Raja Kawas, and Shelia Clancy for support, encouragement, and critical advice during the preparation of the manuscript.

REFERENCES

1. Wood, K., Cornwell, W., and Jackson, J. (2001) Past and future of the mitotic spindle as an onclogy target. *Curr. Opin. Pharmacol. 1*, 370–377.
2. Sakowicz, R., Finer, J. T., Beraud, C., Crompton, A., Lewis, E., Fritsch, A., Lee, Y., Mak, J., Moody, R., Turincio, R., Chabala, J. C., Gonzales, P., Roth, S., Weitman, S., and Wood, K. W. (2004) Antitumor activity of a kinesin inhibitor. *Cancer Res. 64*, 3276–3280.
3. Kapitein, L. C., Peterman, E. J., Kwok, B. H., Kim, J. H., Kapoor, T. M., and Schmidt, C. F. (2005) The bipolar mitotic kinesin Eg5 moves on both microtubules that it crosslinks. *Nature 435*, 114–118.
4. Blangy, A., Arnaud, L., and Nigg, E. A. (1997) Phosphorylation by p34cdc2 protein kinase regulates binding of the kinesin-related motor HsEg5 to the dynactin subunit p150. *J. Biol. Chem. 272*, 19418–19424.
5. Cole, D. G., Saxton, W. M., Sheehan, K. B., and Scholey, J. M. (1994) A "slow" homotetrameric kinesin-related motor protein purified from *Drosophila* embryos. *J. Biol. Chem. 269*, 22913–22916.
6. Kashina, A. S., Baskin, R. J., Cole, D. G., Wedaman, K. P., Saxton, W. M., and Scholey, J. M. (1996) A bipolar kinesin. *Nature 379*, 270–272.
7. Marcus, A. I., Peters, U., Thomas, S. L., Garrett, S., Zelnak, A., Kapoor, T. M., and Giannakakou, P. (2005) Mitotic kinesin inhibitors induce mitotic arrest and cell death in Taxol-resistant and -sensitive cancer cells. *J. Biol. Chem. 280*, 11569–11577.
8. Sharp, D. J., McDonald, K. L., Brown, H. M., Matthies, H. J., Walczak, C., Vale, R. D., Mitchison, T. J., and Scholey, J. M. (1999) The bipolar kinesin, KLP61F, cross-links microtubules within interpolar microtubule bundles of *Drosophila* embryonic mitotic spindles. *J. Cell Biol. 144*, 125–138.
9. DeBonis, S., Simorre, J. P., Crevel, I., Lebeau, L., Skoufias, D. A., Blangy, A., Ebel, C., Gans, P., Cross, R., Hackney, D. D., Wade, R. H., and Kozielski, F. (2003) Interaction of the mitotic inhibitor monastrol with human kinesin Eg5. *Biochemistry 42*, 338–349.
10. Kapoor, T. K., Mayer, T. U., Coughlin, M. L., and Mitchinson, T. J. (2000) Probing spindle assembly mechanisms with monastrol, a small molecule inhibitor of the mitotic kinesin, Eg5. *J. Cell Biol. 150*, 975–988.

11. Maliga, Z., Kapoor, T. K., and Mitchinson, T. J. (2002) Evidence that monastrol is an allosteric inhibitor of the mitotic kinesin Eg5. *Chem. Biol. 9*, 989–996.
12. Mayer, T. U., Kapoor, T. K., Haggarthy, S. J., King, R. W., Schreiber, S. L., and Mitchinson, T. J. (1999) Small molecule inhibitor of mitotic spindle bipolarity identified in a phenotype-based screen. *Science 286*, 971–974.
13. Yan, Y., Sardana, V., Xu, B., Homnick, C., Halczenko, W., Buser, C. A., Schaber, M., Hartman, G. D., Huber, H. E., and Kou, L. C. (2004) Inhibition of a mitotic motor protein: where, how, and conformational consequences. *J. Mol. Biol. 335*, 547–543.
14. Blangy, A., Lane, H. A., d'Herin, P., Harper, M., Kress, M., and Nigg, E. A. (1995) Phosphorylation by p34cdc2 regulates spindle association of human Eg5, a kinesin-related motor essential for bipolar spindle formation in vivo. *Cell 83*, 1159–1169.
15. Sawin, K. E., LeGuellec, K., Philippe, M., and Mitchinson, T. J. (1992) Mitotic spindle organization by a plus-end-directed microtubule motor. *Nature 359*, 540–543.
16. Luo, L., Carson, J. D., Dhanak, D., Jackson, J. R., Huang, P. S., Lee, Y., Sakowicz, R., and Copeland, R. A. (2004) Mechanism of inhibition of human KSP by monastrol: insights from kinetic analysis and the effect of ionic strength on KSP inhibition. *Biochemistry 43*, 15258–15266.
17. Cochran, J. C., Gatial, J. E., Kapoor, T. M., and Gilbert, S. P. (2005) Monastrol inhibition of the mitotic kinesin Eg5. *J. Biol. Chem. 280*, 12658–12667.
18. Cochran, J., and Gilbert, S. P. (2005) ATPase mechanism of Eg5 in the absence of microtubules: insight into microtubule activation and allosteric inhibition by monastrol. *Biochemistry 44*, 16633–16648.
19. Johnson, R. K., McCabe, F. L., Cauder, E., Innlow, L., Whitacare, M., Winkler, J. D., Bergnes, G., Feng, B., Smith, W. W., Morgans, D., and Wood, K. (2002) SB-715992. a potent and selective inhibitor of KSP mitotic kinesin, demonstrates broad-spectrum activity in advanced murine tumors and human tumor xenografts. *Proc. Am. Assoc. Cancer Res. 43*, 1335.
20. Morrison, J. F. (1969) Kinetics of the reversible inhibition of enzyme-catalysed reactions by tight-binding inhibitors. *Biochim. Biophys. Acta 185*, 269–286.
21. Gilbert, S. P., and Mackey, A. T. (2000) Kinetics: a tool to study molecular motors. *Methods 22*, 337–354.
22. Brune, M., Hunter, J. L., Corrie, J. E., and Webb, M. R. (1994) Direct, real-time measurement of rapid inorganic phosphate release using a novel fluorescent probe and its application to actomyosin subfragment 1 ATPase. *Biochemistry 33*, 8262–8271.
23. Cochran, J., Sontag, C. A., Maliga, Z., Kapoor, T. M., Correia, J. J., and Gilbert, S. P. (2004) Mechanistic analysis of the mitotic kinesin Eg5. *J. Biol. Chem. 279*, 38861–38870.
24. Vale, R. D., and Milligan, R. A. (2000) The way things move: looking under the hood of molecular motor proteins. *Science 288*, 88–95.
25. Yang, J. T., Saxton, W. M., Stewart, R. J., Raff, E. C., and Goldstein, L. S. (1990) Evidence that the head of kinesin is sufficient for force generation and motility in vitro. *Science 249*, 42–47.
26. Bergnes, G., Ha, E., Yiannikourous, G., Kalantis, P., Yonce, B. E., and Welday, K. A. (2003) Synthesis of quinazolinones, U.S. Patent WO-03070701.
27. Finer, J. T., Bergnes, G., Feng, B., Smith, W. W., Chabala, J. C., and Morgans, D. J. (2001) Methods and compositions utilizing quinazolinones, U.S. Patent WO-00198278.
28. Cochran, J., Krzysiak, T. C., and Gilbert, S. P. (2006) Pathway of ATP hydrolysis by monomeric kinesin Eg5. *Biochemistry 45*, 12334–12344.
29. Jackson, J. R., Auger, K. R., Gilmartin, A., Eng, W. K., Luo, L., Concha, N., Parrish, C., Sutton, D., Diamond, M., Giardiniere, M., Zhang, S., Huang, P., Belmont, L., Lee, Y., Bergnes, G., Anderson, R., Wood, K. W., and Sakowicz, R. (2005) A Resistance Mechanism for the KSP Inhibitor Ispinesib Implicates Point Mutations in the Compound Binding Site,*AACR-NCI-EORTC* C207.
30. Maliga, Z., Xing, J., Cheung, H., Juszczak, L. J., Friedman, J. M., and Rosenfeld, S. S. (2006) A pathway of structural changes produced by monastrol binding to Eg5. *J. Biol. Chem. 281*, 7977–7982.
31. Kikkawa, M., Sablin, E. P., Okada, Y., Yajima, H., Fletterick, R. J., and Hirokawa, N. (2001) Switch-based mechanism of kinesin motors. *Nature 411*, 439–445.

BI702061G